Available online at www.sciencedirect.com
ScienceDirect
Journal of Power Sources 166 (2007) 430–434
JOURNAL OF POWER SOURCES
www.elsevier.com/locate/jpowsour

Short communication

Effect of cathode inlet manifold configuration on performance of 10-cell proton-exchange membrane fuel cell

Seo Young Kim [a,*], Won Nyun Kim [b]

[a] *Thermal/Flow Control Research Center, KIST, P.O. Box 131, Cheongryang, Seoul 130-650, South Korea*
[b] *R&D Team, VD Division, Samsung Electronics, Suwon 443-742, South Korea*

Received 3 October 2006; accepted 14 December 2006
Available online 21 January 2007

Abstract

A 10-cell proton-exchange membrane fuel cell (PEMFC) stack with 10 cathode flow channels is employed to investigate the effect of airflow inlet manifold configuration on the overall performance. Four different types of airflow inlet manifold with a 90° turn are considered. First, the flow patterns according to the manifold configuration are numerically sought. The computational result for the improved inlet manifold predicts about 8.5% increase in the uniformity of the airflow distribution. The experiments are carried out to confirm the numerical predictions by measuring actual airflow distributions through the fuel cell stack. The polarization curve and the power curve for the 10-cell PEMFC are also obtained to determine the effect of inlet manifold configuration on the actual performance. The maximum power output increases by up to 10.3% on using the improved airflow inlet manifold.

Keywords: Proton-exchange membrane fuel cell; Balance-of-plant; Cathode inlet manifold; Polarization curve; Power; Efficiency

1. Introduction

The efficiency of fuel cells is higher than that of conventional energy converters such as internal combustion engines and gas turbines. In addition, fuel cells are very environment-friendly. For this reason, there has been considerable research on fuel cell stacks and their balance-of-plant (BOP). Among the various types of fuel cell, the proton-exchange membrane fuel cell (PEMFC) is attracting much attention due to its simple structure and easy operation [1].

A single cell of a PEMFC has an output voltage that is too low (typically much less than 1 V due to various losses) for the device to serve as a practical power source. The output voltage is proportional to the number of unit cells connected in series, while the output current depends on the active area of the membrane electrode assembly (MEA) [1,2]. Therefore, a fuel cell is usually composed of a multi-cell stack with a properly sized MEA according to required power output.

For a PEMFC stack, air and fuel (hydrogen) should be supplied through flow-dividing manifold so as to distribute evenly the reactants. As the number of cells increases, however, the flow distribution between them is generally not uniform. The cell with the lowest flow supply determines the overall current limit. Therefore, a uniform flow distribution of air and fuel is crucial for the efficient operation of a PEMFC [3]. In addition, systems with bi-cell stacking also require the uniform airflow distribution for maximum power output [4].

In the present study, the effect of cathode inlet manifold configuration on the overall performance of a 10-cell PEMFC is investigated. Four different types of these manifolds with a 90° turn are considered. The flow distributions according to the inlet manifold configuration are numerically computed and experimentally measured in an actual 10-cell PEMFC. Then, the polarization curve for a 10-cell PEMFC with 10 MEA layers of 50 mm × 50 mm active area is obtained to identify the effect of inlet manifold configuration on the overall performance.

2. Numerical analysis

Air is supplied through an inlet manifold to a 10-cell PEMFC, as displayed in Fig. 1. In the present computations, the problem

* Corresponding author. Tel.: +82 2 958 5683; fax: +82 2 958 5689.
E-mail address: seoykim@kist.re.kr (S.Y. Kim).

0378-7753/$ – see front matter © 2007 Elsevier B.V. All rights reserved.
doi:10.1016/j.jpowsour.2006.12.104

Nomenclature

B	distance between cathode-channels (mm)
D	gap distance of a cathode channel (mm)
H	channel height of inlet manifold (mm)
H_s	streamwise length of stack (mm)
H_t	total length of stack (mm)
I	current (A)
L	width of the stack (mm)
M	mass flow rate of air through cathode per unit depth ($kg\,s^{-1}\,m^{-1}$)
P	power (W)
U	air inlet velocity ($m\,s^{-1}$)

Subscript

ave	average value

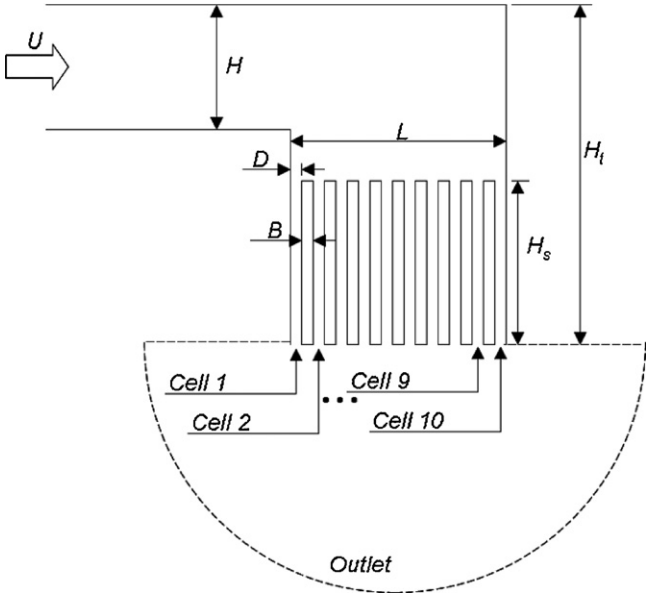

Fig. 1. Schematic of problem and calculation domain.

is assumed to be two-dimensional, incompressible, laminar and steady flow. The dimensions of the computational geometry are identical to the actual 10-cell PEM fuel cell, as depicted in Table 1. The four different types of airflow inlet manifold are displayed in Fig. 2. All the round turns are elliptical.

Based on the conditions for actual PEMFC operation, the inlet air velocity in the manifold was set to $U = 0.57\,m\,s^{-1}$. No-

Table 1
Geometric parameters of channels, manifold and stack

Variables	Value (mm)
B	2.5
D	3.0
H	40.0
H_s	70.0
H_t	160.0
L	52.5

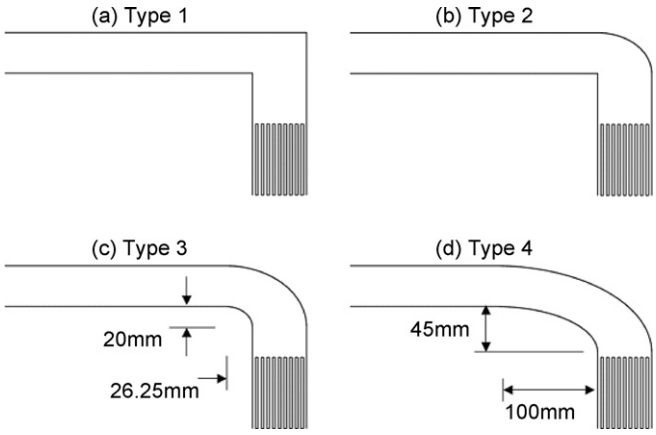

Fig. 2. Cathode inlet manifold configurations: (a) Type 1; (b) Type 2; (c) Type 3; (d) Type 4.

slip conditions were used at all the wall surfaces including those of the stack. At the far downstream outlet, a uniform pressure condition was applied.

In actual PEMFCs, the oxygen concentration decreases and water generation occurs along the cathode channel as a result of the electrochemical reaction. This results in a variation of the air thermophysical properties. In this work, however, attention was focused only on the flow distribution according to the inlet manifold configuration. Therefore, the electrochemical reaction and the variation of air properties were not taken into account.

In an effort to capture the boundary layer flow along both the manifold and the cathode walls, a non-uniform grid network of 100,000 with dense grids near the walls was adopted. The FLUENT software with SIMPLE algorithm was used to obtain solutions for the Navier–Stokes equation [5]. For the discretization of convection terms, the higher order scheme of MUSCL was adopted [6] while the central differencing was used for the diffusion terms.

3. Experimental set-up and procedure

The experimental set-up for the performance measurement of a 10-cell PEMFC consisted of an air supply, a fuel supply, and a fuel cell stack, as shown in Fig. 3. Air was supplied from a compressor through a rectangular Plexiglas duct with multiple mesh layers and a mixing chamber. An inlet manifold with a 90° turn was connected to the end of the duct immediately before the stack. The rate of airflow was controlled by a rotameter and the air temperature was maintained constant by means of an air heater. In the present experiment, the inlet air velocity in the manifold was $U = 0.57\,m\,s^{-1}$ and the air temperature and humidity were kept at 30 °C and 12.0 ± 0.5%, respectively. For measurement of the air velocity distribution in the cathode channel, a hot-wire anemometer (Dantec StreamLine® System) was used.

Fuel (hydrogen) with a purity of 99.999% was supplied to the anode of the stack in the dead-end operation mode [1] via a hydrogen-MFC from a compressed hydrogen tank. A pressure regulator held the internal pressure of the stack to 1.5 bar.

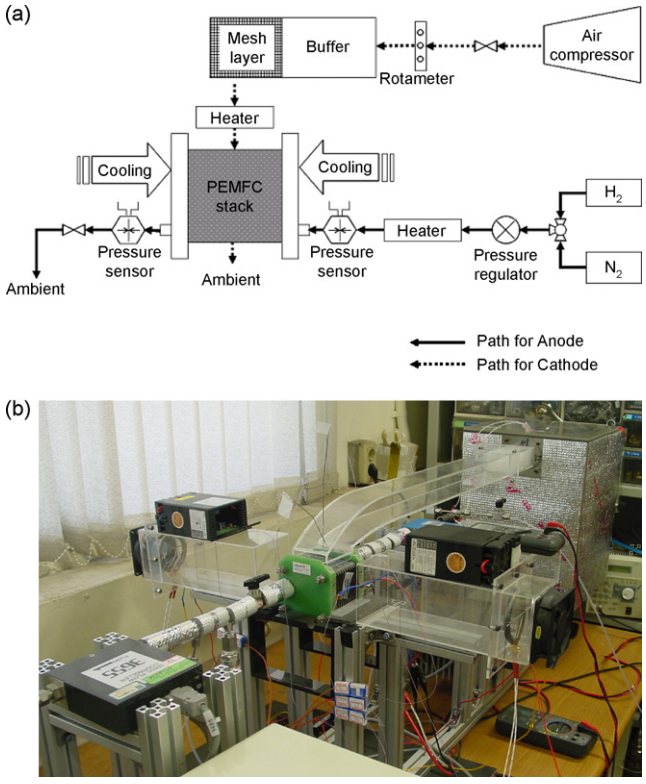

Fig. 3. Experimental set-up: (a) process layout; (b) in perspective.

A NP50 PEMFC stack [heliocentric Energiesysteme, GmbH] was selected for the present experiment. The stack consisted of 10 fuel cells with 10 straight cathode flow channels. The active area of each cell was 25 cm^2 in a square shape. For cooling of the stack during operation or for heating of the stack at start-up, a fan cooling unit with an air temperature controller set to 30 °C was used, as shown in Fig. 3(b).

The following procedure was adopted as a start-up routine [7]. First, nitrogen was used to purge impurities inside the anode channel of the stack. Simultaneously, heated air of 30 °C was directed over the exterior of the stack to enable rapid warm-up. The nitrogen supply was discontinued when the stack temperature reached 30 °C. Hydrogen was fed to the anode and air to the cathode, both in the flow operation mode [1]. In an effort to activate the MEAs inside the stack, the air and the fuel were supplied for 10 min under a current loading of 3 A. Next, the exhaust valve of the anode (dead-end operation mode) was shut and the internal pressure was maintained at 1.5 bar. Finally, experiments were performed to obtain the polarization curve for the stack.

The following procedure was taken to obtain the polarization curve. Hydrogen was supplied in the dead-end operation mode and air in the flow operation mode under no external current loading. After reaching a steady state, the open-circuit voltage (OCV) was measured. The current loading was increased to a specific value. Again, the voltage output was determined from the stack in the steady state. A polarization curve was obtained for various current loading conditions.

After finishing the experiment, the following closing-down operation was taken to prevent any deterioration of MEA performance due to crossover of hydrogen that was unused at the anode. The external loading was removed, the hydrogen supply was shutoff, the exhaust valve of the anode was opened and nitrogen supplied for purging. Simultaneously, the air supply was shutoff. Air from the cooling device cooled down the stack until the temperature reached the ambient value.

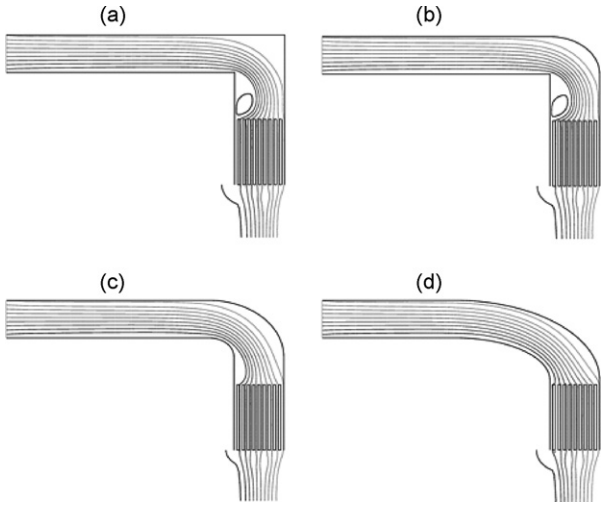

Fig. 4. Streamline patterns: (a) Type 1; (b) Type 2; (c) Type 3; (d) Type 4.

4. Results and discussion

The effect of cathode inlet manifold configuration on the flow distribution through the 10-cell stack is presented in Figs. 4–6. The data were obtained by compiling the computational results.

The computational streamlines for various manifold configurations are displayed in Fig. 4. The airflows through the inlet manifold with a 90° turn and then passes through 10 cathode channels. For the Type 1 manifold with sharp inner and outer turns, a large flow separation occurs at the inner wall just behind the 90° turn inside the manifold. For the Type 2 inlet manifold with a smooth turn at the outer wall and a sharp turn at the inner

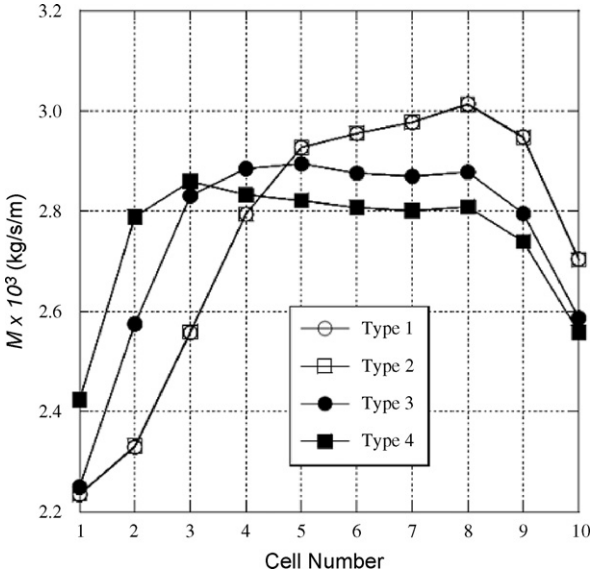

Fig. 5. Computational airflow distributions for various inlet manifolds.

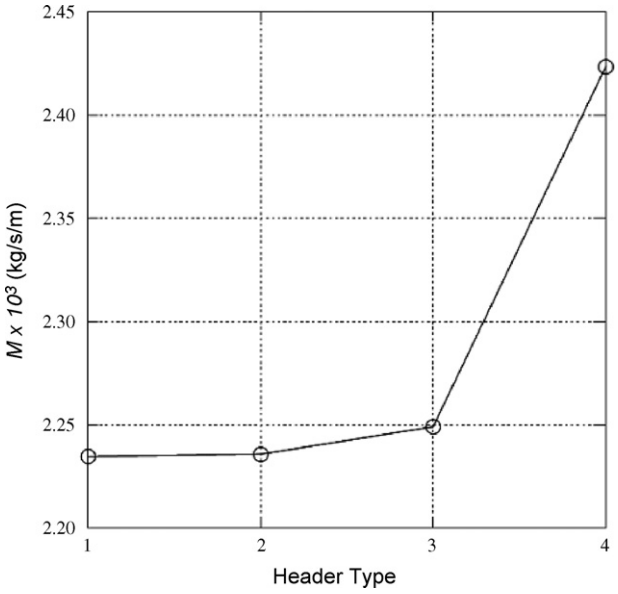

Fig. 6. Airflow rate through first cell.

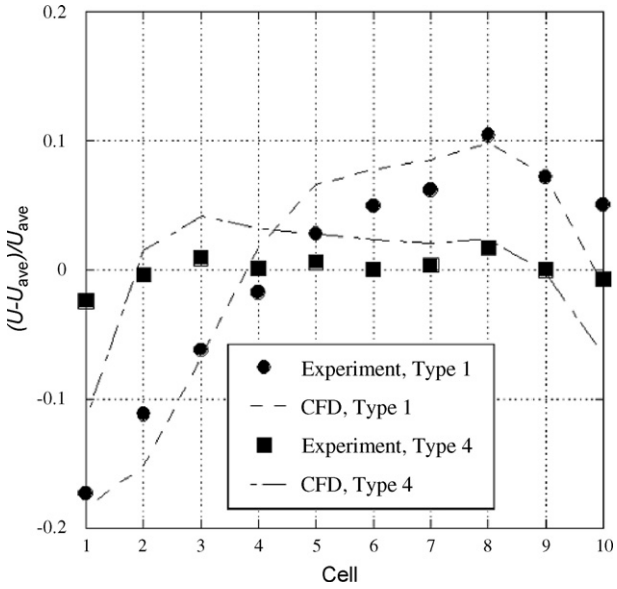

Fig. 7. Comparison of airflow distribution between computations and experiments.

wall, flow separation still occurs so that the pattern inside the manifold is little improved. When the inner wall is changed to an elliptic round shape, as displayed in Fig. 4(c) and (d), the flow separation totally disappears. The flow pattern is more improved for Type 4 with a much smoother turn at the inner wall. It is also noted that the ambient air entrains near the discharging exit of the stack.

The computational airflow distribution according to the inlet manifold configuration is given in Fig. 5. As anticipated, the airflow rate is the lowest at the first cathode channel for all the manifolds. It is noticeable that the Type 2 manifold with a round turn only at the outer wall shows no improved flow distribution compared with the Type 1 manifold. This implies that the flow separation still found in the Type 2 manifold has a strong impact on the overall flow distribution. By contrast, the manifold types with a round turn (Types 3 and 4) display a more uniform flow distribution along the cells and an increased airflow rate at the first cathode channel. The increase in airflow at the first cathode channel is very favourable in terms of the overall cell performance because the cell with the lowest airflow rate limits the overall current.

The rate of airflow supplied to the first cathode channel is given in Fig. 6. The manifolds with improved configurations (Types 3 and 4) provide substantially increased airflow rates due to the suppression of flow separation at the inner wall. Type 4 manifold supplies 8.5% more airflow to the first channel compared with the Type 1 manifold.

A comparison of the airflow distribution obtained from computational results and experimentally measured data is made in Fig. 7. Although small quantitative discrepancy is found, the overall pattern of the flow distribution is in reasonably good agreement. For the Type 1 manifold, the maximum flow rate experimentally measured is achieved at the eighth cell, which is in excellent coincidence with the computational result. For the Type 4 manifold, the measured airflow rate at the first cathode channel is slightly higher and the measured flow distribution is more uniform than the computational result. This may be attributed to the use of two-dimensional computations.

The polarization curves measured for the NP50 stack according to the inlet manifolds are shown in Fig. 8. The polarization curves are typical of those reported for PEMFCs [1,2]. At low a current loading, the output voltage quickly falls as the current loading increases (i.e., activation polarization takes place). At a moderate current loading, the voltage output linearly decreases with increase in current (i.e., the ohmic polarization). Further increase in current loading results in a sudden fall in output voltage (i.e., concentration polarization). The improved manifolds of Types 2–4 provide better performance, namely, higher voltages at moderate and high current loadings compared with

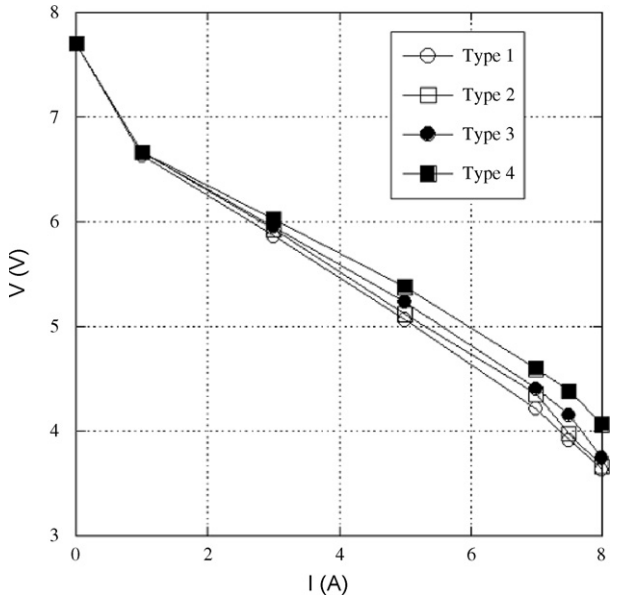

Fig. 8. Polarization curves.

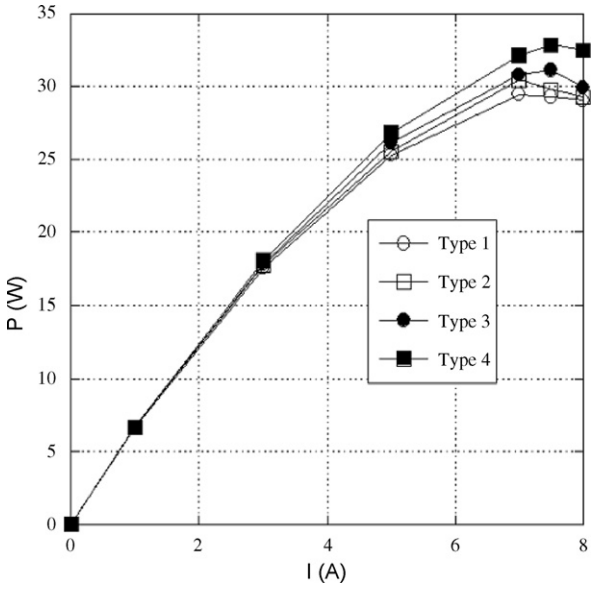

Fig. 9. Power curves.

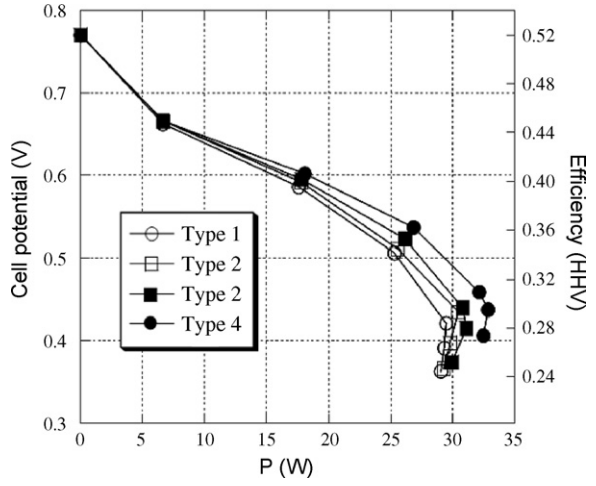

Fig. 10. Fuel cell efficiency vs. power.

the Type 1 manifold. It should be noted that the more uniform the flow distribution, the better is the fuel cell performance.

The power output from the NP50 fuel cell as a function of current loading is given in Fig. 9. Maximum power is obtained at a current loading of around 7 A, irrespective of the manifold type. At low current loadings up to 3 A, the power output is little affected by the manifold type. On the other hand, the power output deviates considerably at higher current loadings. The Type 4 manifold shows a 10.3% increase in maximum power output over that obtained with the Type 1 manifold.

The fuel cell efficiency, based on the higher heating value (HHV) of hydrogen, as a function of power output is plotted in Fig. 10. A maximum power of 32.8 W is reached at an efficiency of 30% for the Type 4 manifold. Meanwhile, a Type 1 manifold yields the maximum power of 29.5 W at an efficiency of 28%. Therefore, it should be noted that the improved manifold yields increased cell potential, increased power output, and higher fuel cell efficiency. From data in Fig. 10, it is seen that a higher cell efficiency may be obtained at a very low power output. Nevertheless, this requires a larger fuel cell stack for the same power output, which is not useful in an engineering sense. Furthermore, hydrogen crossover and internal current losses can be serious at a very low current loading [1].

5. Conclusions

The present study has investigate the effect of cathode inlet manifold configuration on the overall performance of a 10-cell PEMFC. An improved manifold configuration eliminates the flow separation that occurs at the inner wall in a manifold with a 90° turn. As a result, it provides an 8.5% more uniform flow distribution. The polarization curve and the corresponding power curve are also strongly influenced by the inlet manifold configuration. The improved airflow distribution results in increased cell potential, increased power output, and higher fuel cell efficiency. The maximum power output is increased by 10.3% when using the improved airflow inlet manifold.

Acknowledgements

The authors are grateful to Mr. Y. H. Kim for assistance with the experimental setup. This work was supported by research grant No. 2E19320 of the Korea Institute of Science and Technology, Seoul, South Korea.

References

[1] F. Barbir, PEM Fuel Cells: Theory and Practice, Elsevier Academic Press, 2002.
[2] J. Larminie, A. Dicks, Fuel Cell Systems Explained, John Wiley & Sons Ltd., 2003.
[3] G. Mohan, B.P. Rao, S.K. Das, S. Pandiyan, N. Rajalakshmi, K.S. Dhathathreyan, ASME Trans., J. Energy Resour. Technol. 126 (2004) 262–270.
[4] W. Qian, D.P. Wilkinson, J. Shen, H. Wang, J. Zhang, J. Power Sources 154 (2006) 202–213.
[5] Fluent 6.2 User's Guide, Fluent Inc., 2004.
[6] B. van Leer, J. Comp. Phys. 32 (1979) 101–136.
[7] Operating Instructions, NP50 Fuel Cell Stack, heliocentris Energiesysteme GmbH, Berlin, 2000.